The Calculated Evolution of the Plasma Channel in the Electric Discharge in SF_6[1]

A.G. Yastremskii and Yu.I. Bychkov

Institute of High-Current Electronics SB RAS, 2/3, Academichesky ave., Tomsk, 634055, Russia
E-mail: yastrems@lgl.hcei.tsc.ru

Abstract – The simulation of the kinetic processes in the spatially homogeneous and heterogeneous plasma of the gas discharge in SF6 is performed. The spatial heterogeneities of the discharge are simulated in the framework of a self-consistent 2D model. The calculated time dependences of the rates of the most important processes and the concentrations of electrons, ions, concentration of vibration exited $SF_6(v)$, molecules SF_6^* in electronically exited levels, and other particles that affect the plasma characteristics are presented. The kinetic processes are analyzed and their effect on the plasma characteristics is demonstrated. An increase in the conductivity inside the channel is discussed. The results of the calculation illustrate the dynamics of the spatial structure of discharge in SF_6.

1. Introduction

The urgency of investigation of discharge properties in the gas mixtures based on SF_6 is caused by wide application of the mixtures based on this gas in electronic and switching equipment as well as in the pulsed electric-discharge HF/DF lasers that are the promising sources of coherent radiation for technological applications. The discharges of this type are noted for a change in a space structure, formation of plasma channels, broadening or narrowing of the discharge sectional area. The discharge-width change effect was observed in [1–5].

Mechanisms of the discharge width change and plasma channel formation in SF_6-based mixtures remain obscure and require further detailed investigation. We have created a 2D-model for discharges in SF_6 and for gas mixtures containing SF_6. Description of a model and preliminary obtained results were published in the following papers [6-7].

The present paper presents the results of numerical calculations of a plasma channel development. Calculated time dependences have been obtained for electron concentrations, SF_6^*-molecules at electron levels and $SF_6(v)$-molecules with excitation at the oscillating levels. The frequencies of the processes of direct and stepwise ionization were considered in detail as well as the frequencies of electron attachment to SF_6-molecules in the ground state and to $SF_6(v)$-molecules with excitation at the oscillating levels. Analysis of physical processes influencing the plasma channel formation was made.

2. Discharge model

Simulation of a plasma channel development was made on the basis of a self-consisted two-dimensional (2D) model. Cathode spots and processes on the cathode surface were not taken into account. To initiate a plasma channel development, the initial non-uniform electric field was created in a discharge gap. A metallic half-sphere-shaped non-uniformity with a characteristic spatial scale of 0.1 cm was placed in the cathode center, Fig. 1. The non-uniformity initiated the plasma channel development along the gas spacing axis. The cross sections of the electron interaction with the components are taken from [8].

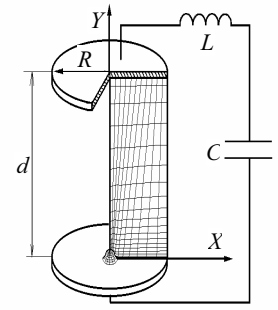

Fig. 1. Electric circuit and discharge gap geometry: $d = 2.5$ cm; $R = 2.3$ cm; $S = 17.0$ cm^2; $C = 36$ nF; $L = 9.2$ nH; $U_0 = 24$ kV; $P = 60$ Torr

There are three characteristic regions in the gas spacing under consideration. Electron concentration was maximal at the cathode, in the region of non-uniformities. The channel was broadening in the direction from the cathode to the anode and electron concentration in the anode region was considerably less than in the cathode region. The third region included an undisturbed uniform discharge in the rest part of the gas spacing.

The main problem of numerical simulations was to find out kinetic processes influencing the formation of the plasma channel that was developing simultaneously with a uniform discharge in the rest part of the volume.

One of the main approximations of a 2D-model was a condition for the local character of the electric

[1] The research has been carried out with the support of RFBR (Grant No. 07-08-00197-a).

field that practically means that the constants of reactions with participation of electrons and transport coefficients at each point of the discharge depend only on the electric field strength value at a given point. At each point of the computational mesh the Boltzmann equation was solved taking into account all channels of energy losses by electrons and a system of balanced equations was solved as well. An electric-field **E** was determined from the current continuity equation:

$$\mathrm{div}(\mathbf{j}) = e\mu(n_e \mathrm{div}(\mathbf{E}) + \mathbf{E}\,\mathrm{grad}(n_e)) = 0. \qquad (1)$$

Here, **j** is the discharge current density, e, μ, *n* are the electron charge, mobility, and concentration, respectively. The system of balanced equations was solved by Gear method, equation (1) was solved by the weighted residual method using curvilinear nonorthogonal computational mesh.

3. Calculation results

Figure 1 presents the discharge gap circuit and initial discharge conditions. The non-uniformity geometry at the cathode was chosen so that maximum field strength near the cathode exceeded threefold (28 kV/cm) the field in the uniform region of the gap. The choice is caused by the fact that at a less field strength the channel is not developing.

Figure 2 presents the waveforms of plasma voltage, total discharge current, channel current, and current of plasma in the undisturbed discharge region. Plasma voltage begins decreasing from 24 kV to 20 kV during 10 ns owing to high rate of current rise and voltage increase at the inductance. In this discharge stage the channel current rises more rapidly than in the rest part of the volume. At further development, the channel current has an oscillating character. In the undisturbed region, a small oscillation is observed as well at the current at its maximum value. The total discharge current rises monotonously and decays.

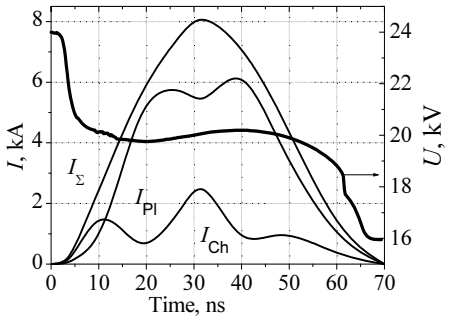

Fig. 2. Waveforms of plasma voltage, total discharge current I_Σ, channel current I_{Ch}, and I_{Pl} current of plasma in the undisturbed discharge region

Figure 3 presents the discharge spatial structure for different moments of time. The current lines are used that constructed so that an equal portion (~ 1% in a given case) of a total current that flows through the whole layer is flowing between two neighboring lines. The more is the density of the lines, the higher are the current density and discharge power density. This figure shows a piece of the discharge gap of the radius 1.0 cm; the discharge is burning in a volume of the radius 2.5 cm. The channel sectional area equals to a small part of the total sectional area of the discharge.

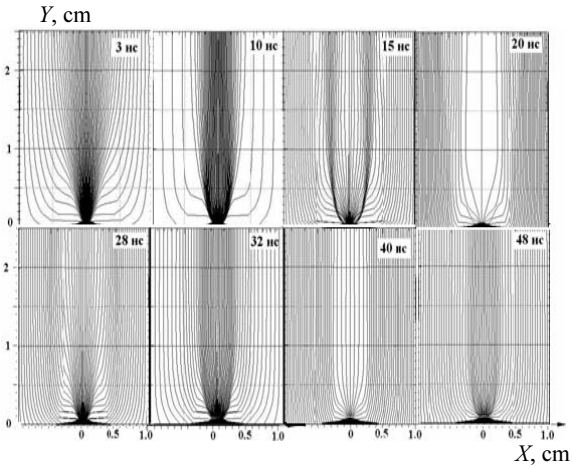

Fig. 3. Current distribution (current lines) by discharge gap cross-section at different moments of time. A fragment of a 1.0-cm-radius gas gap is presented. Electrode radius is 2.3 cm

A plasma channel begins its formation 2 ns (Fig. 3) after the discharge initiation. The channel diameter in the non-uniformity region at this moment of time equals to ~ 2 mm and practically has no changes later. The channel diameter in the anode region is d ≈ 8 mm at t = 3 ns. The plasma channel formation comes to an end at t = 10 ns. At that moment of time, the greater part of the discharge current is flowing through the plasma channel. The channel diameter in the anode region decreases to ~ 6 mm and the cross-sectional area decreases to S = 0.28 cm^2, respectively, that equals to ≈ 2% of the total discharge area. At this moment of time, the current density in the channel is much greater than the current density of the gas volume undisturbed part.

Figure 4 presents the time variation of electron concentration for three regions of the gas gap, namely: in the non-uniformity region at the cathode, at the discharge axis in the anode region, and in the undisturbed discharge region.

The data in Figs. 2, 3, and 4 give a full conception of time variation for the spatial structure of the discharge. After 10 ns, the total discharge current continues growing, the current in the uniform discharge region increases, the channel current decreases and the electron concentration in the channel decreases as well. By the time moment of 20 ns, the channel current becomes minimal. In the time lag from 10 to 20 ns the electron concentration in the channel decreases (Fig. 4) by 15 times. Afterwards, two more current oscillations take place in the channel.

A tendency is that after initial formation of the plasma channel it vanishes and appears again with a

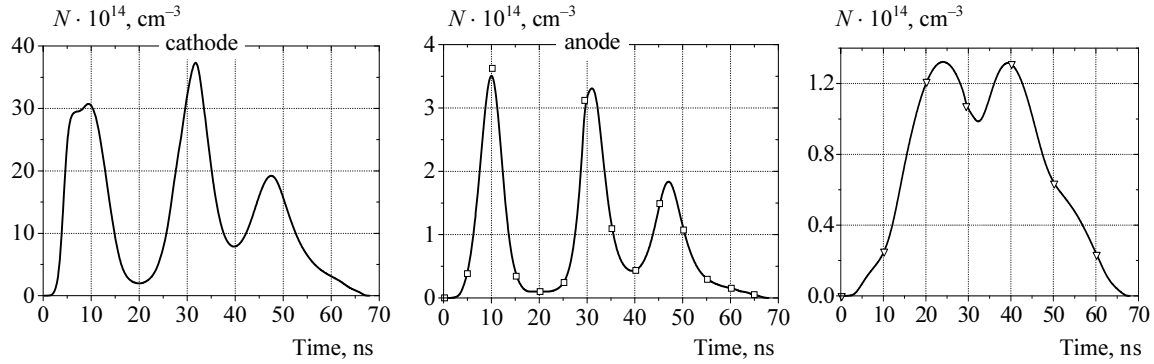

Fig. 4. Electron concentration versus time in the region of cathode non-uniformity (*a*), anode region (*b*), and undisturbed undisturbed discharge region (*c*)

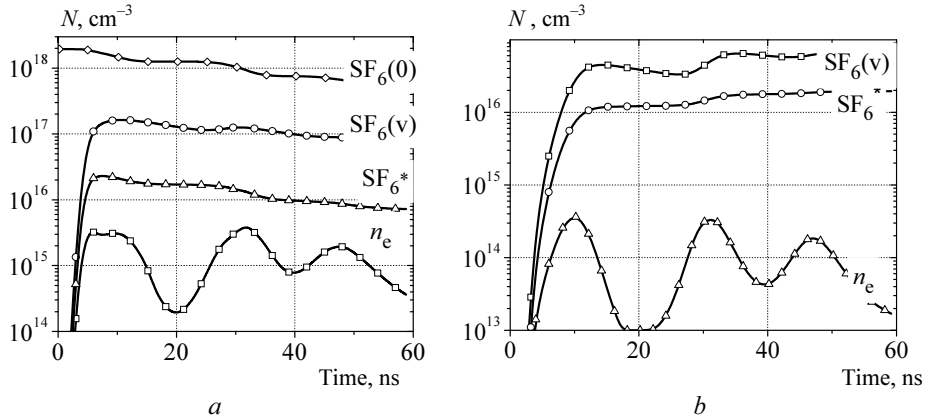

Fig. 5. Concentrations of n_e, $SF_6(v)$, and SF_6^* versus time: *a* – cathode region; *b* – anode region

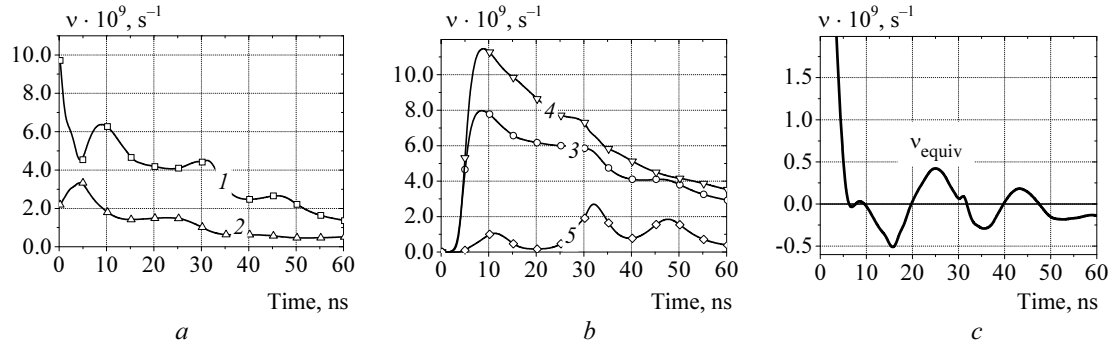

Fig. 6. *1* – $SF_6(0)$ ionization frequency, *2* – frequency of attachment to $SF_6(0)$ (*a*); *3* – SF_6* ionization frequency, *4* – frequency of attachment to $SF_6(v)$, *5* – recombination frequency (*b*); ν_{equiv} – equivalent frequency. Cathode region (*c*)

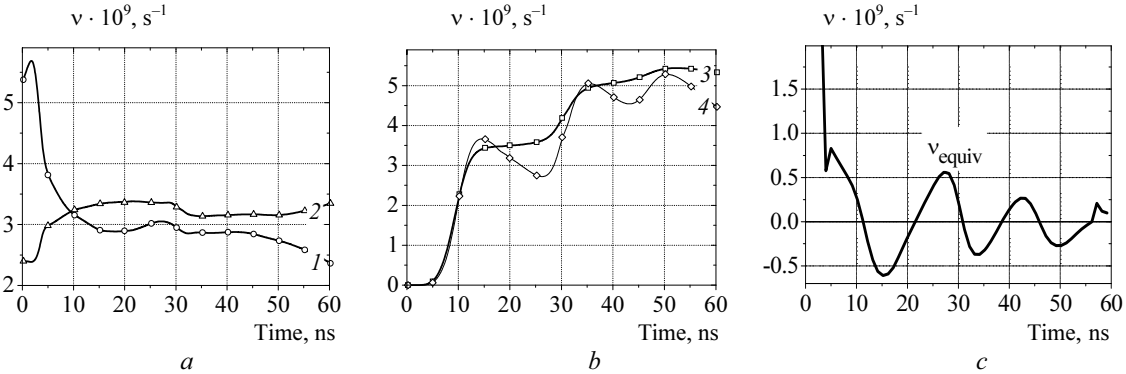

Fig. 7. *1* – $SF_6(0)$ ionization frequency, *2* – attachment to $SF_6(0)$ (*a*); *3* – of SF_6^* ionization frequency. *4* – frequency of attachment to $SF_6(v)$ (*b*); ν_{equiv} – equivalent frequency. Anode region (*c*)

period of ~ 20 ns. Each time at the plasma channel formation some part of the total discharge current flowing through the channel decreases gradually. The discharge space structure becomes even.

4. Discussion of calculation results

Production of electrons occurs in the processes of direct ionization of SF_6-moleculs and step ionization of SF_6^*-molecules with electron-level excitation. Electron death occurs in the processes of attachment to SF_6-molecules in the ground state, attachment to SF_6(v)-molecules with excitation at the oscillating levels as well as in the processes of electron-ion recombination. Two processes are functioning at small concentration of electrons $n_e < 10^{13}$ cm^{-13} in plasma, namely: direct ionization and electron attachment to SF_6-molecules in the ground state. Frequencies of these processes depend on the electric field strength. Ionization decreases and attachment increases at the electric field reduction.

Electron concentration rise leads to increase of concentration of excited SF_6^*- and SF_6(v)-molecules resulting in the growth of frequencies of the step ionization, electron attachment to SF_6(v)-molecules and electron-ion recombination. These frequencies weakly depend on the field strength and depend mainly on the electron concentration. Rise of these frequencies results in essential changes of discharge time and spatial responses.

Figure 5 presents time dependences of n_e, SF_6(v), SF_6^*, and SF_6(0) concentrations for two points disposed at the cathode and anode of the channel axis. Electron concentration at the cathode is higher by an order than at the anode and oscillating character of dependence is preserved at both the cathode and anode. Concentration of SF_6(0) at the cathode diminishes while concentration of these molecules at the anode changes negligibly. Strong rise of SF_6(v) and SF_6^* concentrations occurs at the discharge start, approximately during first ten nanoseconds. Concentration of SF_6^*-molecules is higher by an order and concentration of SF_6(v) is higher by two orders of magnitude than electron concentration, respectively. Concentration of these molecules in the time interval equals to 30 ns (the time between two maxima of electron concentration) decrease approximately twice relative their maximal values. The change of SF_6(v) and SF_6^* concentrations results, respectively, in the frequency change of the step ionization and electron attachment to SF_6(v)-molecules. The losses of the excited atoms of SF_6(v) and SF_6^* occur mainly in the quenching reactions at their collisions with plasma particles, including electrons as well.

Figs. 6, *a* and *b* present time dependences of electron production and death frequencies in the cathode non-uniformity region. Fig. 6, *c* presents the time dependence of the equivalent frequency that is equal to the difference of frequencies of a total ionization and total frequency of attachment and recombination. An equivalent frequency is the frequency of electron concentration change. As it follows from Fig. 6, *c*, this frequency makes oscillations in time relative zero and equals to zero at the moment of time equal to 10, 20, 30, and 40 ns. This corresponds to the minimum and maximum values of electron concentration in Fig. 4, *a*.

Figs. 7 (*a*, *b*, and *c*) presents time dependences of electron production and death frequencies in the channel for anode region. The component frequencies (Figs. 7, *a* and *b*) differ from the frequencies for the cathode region presented in the previous figure. Equivalent frequencies both for the cathode and anode regions have an oscillating character and remain practically equal except small differences. Comparison of the equivalent (Fig. 7, *c*) and attachment (Fig. 7, *b*) frequencies results in conclusion that oscillations of these frequencies occur in an antiphase. Minimum (maximum) values of the equivalent frequency correspond to maximum (minimum) values of the attachment frequency. The total attachment frequency makes oscillations relative the total ionization frequency. This makes time oscillation of electron concentration.

In the mode under consideration, in which two discharges differing in the frequencies of kinetic processes are developed simultaneously in a gas gap, there are two mechanism of frequency matching that operates in each of these discharges. The first mechanism realizes matching of the total discharge current rise rate and plasma voltage. Current growth rate results in the plasma voltage reduction. The second mechanism realizes matched distribution of the field strength and electron concentration in space and time in a non-uniform channel discharge according to the current continuity principle. Monotonous rise and decay of the total current provides the first mechanism. Total current distribution between the channel and the rest part of the volume provides the second mechanism.

References

[1] V.V. Apollonov, A.A. Belevtsev, S.Yu. Kazantsev et al., Kvant. Elektron. **32**, 92 (2003)

[2] Yu. Bychkov, S. Gortchakov, and A. Yastremskii, Kvant. Elektron. **30**, 733 (2000).

[3] V.V. Apollonov, A.A. Belevtsev, K.N. Firsov, S.Yu. Kazantsev, and A.V. Saifulin, Kvant. Elektron. **30**. 207–214 (2000).

[4] Yu. Bychkov, S. Gortchakov, B. Lacour, et al., J. Phys. D: Appl. Phys. **36**, 380 (2003).

[5] Yu. Bychkov, S. Gortchakov, B. Lacour, S. Pasquiers, C. Postel, V. Puech, and A. Yastremsky, SPIE Proc. **4747**, 262–271 (2002).

[6] Yu.I. Bychkov, S.A. Yampolskaya, and A.G. Yastremsky, Izv. Vyssh. Uch. Zav., Fizika, No. 11, Appendix C., 496–500 (2006).

[7] Yu. Bychkov, S.A. Yampolskaya, and A.G. Yastremsky, Izv. Vyssh. Uch. Zav., Fizika **50**, 236–240 (2007).

[8] L.G. Christophorou and J. Olthoff, J. Phys. Chem. Ref. Data **29**, 267 (2000).